ERG promotes the maintenance of hematopoietic stem cells by restricting their differentiation

Kasper Jermiin Knudsen,[1,2,3,7] Matilda Rehn,[1,2,3,7] Marie Sigurd Hasemann,[1,2,3] Nicolas Rapin,[1,2,3,4] Frederik Otzen Bagger,[1,2,3,4] Ewa Ohlsson,[1,2,3] Anton Willer,[1,2,3] Anne-Katrine Frank,[1,2,3] Elisabeth Søndergaard,[1,2,3] Johan Jendholm,[1,2,3] Lina Thorén,[1,2,3] Julie Lee,[1,2,3] Justyna Rak,[5] Kim Theilgaard-Mönch,[1,2,6,8] and Bo Torben Porse[1,2,3,8]

[1]The Finsen Laboratory, Rigshospitalet, Faculty of Health Sciences, University of Copenhagen, DK-2200 Copenhagen N, Denmark; [2]Biotech Research and Innovation Centre (BRIC), University of Copenhagen, DK-2200 Copenhagen N, Denmark; [3]Danish Stem Cell Centre (DanStem) Faculty of Health Sciences, University of Copenhagen, DK-2200 Copenhagen N, Denmark; [4]The Bioinformatic Centre, Department of Biology, Faculty of Natural Sciences, University of Copenhagen, DK-2200 Copenhagen N, Denmark; [5]Molecular Medicine and Gene Therapy, Lund Stem Cell Center, Lund University, SE-22184 Lund, Sweden; [6]Department of Hematology, Skånes University Hospital, University of Lund, SE-22185 Lund, Sweden

The balance between self-renewal and differentiation is crucial for the maintenance of hematopoietic stem cells (HSCs). Whereas numerous gene regulatory factors have been shown to control HSC self-renewal or drive their differentiation, we have relatively few insights into transcription factors that serve to restrict HSC differentiation. In the present work, we identify ETS (E-twenty-six)-related gene (ERG) as a critical factor protecting HSCs from differentiation. Specifically, loss of *Erg* accelerates HSC differentiation by >20-fold, thus leading to rapid depletion of immunophenotypic and functional HSCs. Molecularly, we could demonstrate that ERG, in addition to promoting the expression of HSC self-renewal genes, also represses a group of MYC targets, thereby explaining why *Erg* loss closely mimics *Myc* overexpression. Consistently, the BET domain inhibitor CPI-203, known to repress *Myc* expression, confers a partial phenotypic rescue. In summary, ERG plays a critical role in coordinating the balance between self-renewal and differentiation of HSCs.

[*Keywords*: hematopoietic stem cell; ERG; MYC; differentiation; self-renewal; CPI-203]

Supplemental material is available for this article.

Received July 7, 2015; revised version accepted August 27, 2015.

Hematopoietic stem cells (HSCs) are essential for the lifelong production of blood cells, and careful regulation of their numbers is required for the daily replenishment of aged and defective cells. HSCs have therefore developed intricate molecular networks in order to balance precisely their cellular fate choices, including their propensities to maintain quiescence, proliferate, die, and differentiate, all with the purpose of maintaining hematopoietic homeostasis. Importantly, disturbances in any of these fate options may lead to alterations in HSC numbers that may ultimately result in a decline in hematopoietic output or set the stage for malignant transformation.

HSC fate options are controlled by numerous molecular pathways that in turn are affected by signals from the bone marrow (BM) microenvironment (i.e., the HSC niche) as well as intrinsic regulators, including transcription factors (Rossi et al. 2012). Numerous studies in mice have identified factors that support self-renewal, including C/EBPα, c-MYB, and SATb1 (Lieu and Reddy 2009; Will et al. 2013; Hasemann et al. 2014). Other factors, such as DNMT3a, shown to restrict self-renewal, are equally prevalent (Challen et al. 2012). Similarly, several studies have identified factors that appear to promote differentiation, including the well-studied oncogene MYC. Here, the conditional loss of *Myc* leads to a block in differentiation and accumulation of HSCs, whereas overexpression of *Myc* promotes HSC differentiation at the expense of self-renewal (Wilson et al. 2004). Finally, epigenetic regulators such as BMI-1 and TET2 have been reported to prevent HSC differentiation. (Iwama et al. 2004; Ko et al. 2011; Moran-Crusio et al. 2011; Quivoron et al. 2011).

[7]These authors contributed equally to this work.
[8]These authors contributed equally to this work.
Corresponding author: bo.porse@finsenlab.dk
Article is online at http://www.genesdev.org/cgi/doi/10.1101/gad.268409.115.

The E-twenty-six (ETS)-related gene (ERG) is a member of the ETS family of transcription factors, of which several, including PU.1, have been shown to play a role in HSC maintenance (Loughran et al. 2008; Ng et al. 2011). *Erg* was identified in a sensitized genetic screen as a gene involved in HSC function, and the molecular defect was assigned to a point mutation in the DNA-binding domain of ERG (Loughran et al. 2008). $Erg^{Mld2/+}$mice (i.e., heterozygous carriers of the mutant *Erg* allele) had slightly reduced numbers of immunophenotypical HSCs that appeared functionally compromised in transplantation experiments. In addition, follow-up work demonstrated that although *Erg* haploinsufficiency was compatible with lifelong HSC self-renewal, it strongly impaired stress hematopoiesis following exposure to myelotoxic treatment (Ng et al. 2011). Collectively, these data suggest that ERG could be particularly important during the expansion of HSCs. This notion gained further credibility from studies of the role of ERG during fetal hematopoiesis (Taoudi et al. 2011). Using $Erg^{Mld2/Mld2}$ embryos as a model, ERG was shown to be dispensable for primitive hematopoiesis as well as HSC emergence. In contrast, ERG was found to be essential during the early phases of definitive hematopoiesis, which entail the expansion and maintenance of HSCs. Finally, evidence was provided for the direct ERG-dependent control of *Gata2* and *Runx1* expression, two well-known players of various aspects of HSC biology (Ichikawa et al. 2004, 2008; Rodrigues et al. 2005).

Although these studies provide ample evidence for a functional role of ERG in HSC biology, they also raise a number of additional questions, especially pertaining to the molecular consequences of the ERG variant. The *Mld2* mutation mapped to the DNA-binding domain of ERG; however, it did not interfere with DNA binding per se but instead interfered with the transcriptional activity of the protein. As ETS family members share similar, albeit not identical, DNA recognition motifs, the *Mld2* variant could in principle act as dominant-negative by interference with the activity of other ETS family members of known importance in hematopoiesis (Wei et al. 2010). These issues could be resolved by the development of a conditional *Erg* knockout allele, which would allow the assessment of ERG function without any confounding impact on the function of other ETS factors.

Several factors known to be important in HSC biology have also been reported to play roles in the maintenance or development of leukemic stem cells. Indeed, we demonstrated recently that the myeloid tumor suppressor C/EBPα is essential for HSC maintenance as well as the initiation of mixed-lineage leukemia (MLL)-rearranged acute myeloid leukemia (AML) (Hasemann et al. 2014; Ohlsson et al. 2014). Similarly, ERG has also been demonstrated to have an impact on the characteristics of leukemia development/maintenance in a number of settings. *ERG* is frequently overexpressed in human AML and T-cell acute lymphoblastic leukemia (T-ALL) and is associated with poor outcome in these leukemias (Marcucci et al. 2005, 2007; Baldus et al. 2006). In mice, ectopic expression of *Erg* can lead to the development of either T-ALL through the acquisition of *Notch1* mutations or a condition resembling acute megakaryocytic leukemia associated with Down syndrome (DS-AMKL) (Salek-Ardakani et al. 2009; Tsuzuki et al. 2011; Carmichael et al. 2012). The latter is of particular interest, as *ERG* is located on chromosome 21 and thus is amplified in individuals with Down syndrome. Finally, ectopic expression of ERG has been shown to promote the execution of a transcriptional program resembling that of human AML stem cells and progenitors (Goldberg et al. 2013). However, despite the strong evidence that ERG can promote the onset of several types of human leukemia, no reports have addressed whether ERG is actually required for this process.

Here we set out to characterize the requirement of ERG for HSC function and for the development of leukemia using a newly generated mouse line that allows for the conditional ablation of the DNA-binding domain of ERG. Using this model, we could show that ablation of ERG function promotes the rapid loss of self-renewing HSCs. Moreover, analysis of HSC population dynamics following *Erg* ablation combined with mathematical modeling demonstrates that ERG is required to prevent HSCs from differentiating prematurely. Interestingly, we could show that this is associated with the up-regulation of an MYC-dependent transcriptional program and that ERG binds to MYC target genes, suggesting that ERG restricts HSC differentiation through repression of MYC activity. Consistently, the phenotype could be partially rescued by pharmacological down-regulation of MYC levels in vivo. In contrast to the pronounced importance of ERG in HSCs, the protein is largely dispensable for both myeloid and lymphoid transformation, pointing to a unique role for ERG in normal stem cell biology.

Results

Conditional deletion of Erg *results in a massive loss of BM cells*

In order to investigate the importance of ERG for adult hematopoiesis, we flanked exon 11, encoding the DNA-binding Ets domain, with LoxP sites, thereby generating a mouse line allowing for the functional ablation of ERG (Fig. 1A). The resultant Erg^{fl} animals were subsequently crossed into the *Mx1Cre* strain, resulting in the generation of $Erg^{fl/fl}$; *Mx1Cre* animals in which ERG function can be efficiently abolished in hematopoietic cells following polyinosinic:polycytidylic acid (pIpC)-mediated activation of the Cre recombinase. Specifically, pIpC injections led to the essentially complete deletion of *Erg*, as assessed by PCR-based genotyping of BM cells (Fig. 1B) and quantitative RT–PCR (qRT–PCR) analysis of *Erg* expression in FACS-sorted multipotent progenitor (MPP) cells (LSK $CD150^{-}$ $CD48^{+}$) (Fig. 1C).

We first assessed the functional consequences of *Erg* deletion 2 wk (15 d) and 4 wk following pIpC injection and found a substantial reduction of BM cells in *Erg*-deleted ($Erg^{\Delta/\Delta}$) mice versus $Erg^{fl/fl}$ littermate controls (Fig. 1D). *Erg* is predominantly expressed in immature hematopoietic cells (Supplemental Fig. S1A), and we consistently found the numbers of megakaryocytic, erythroid, and

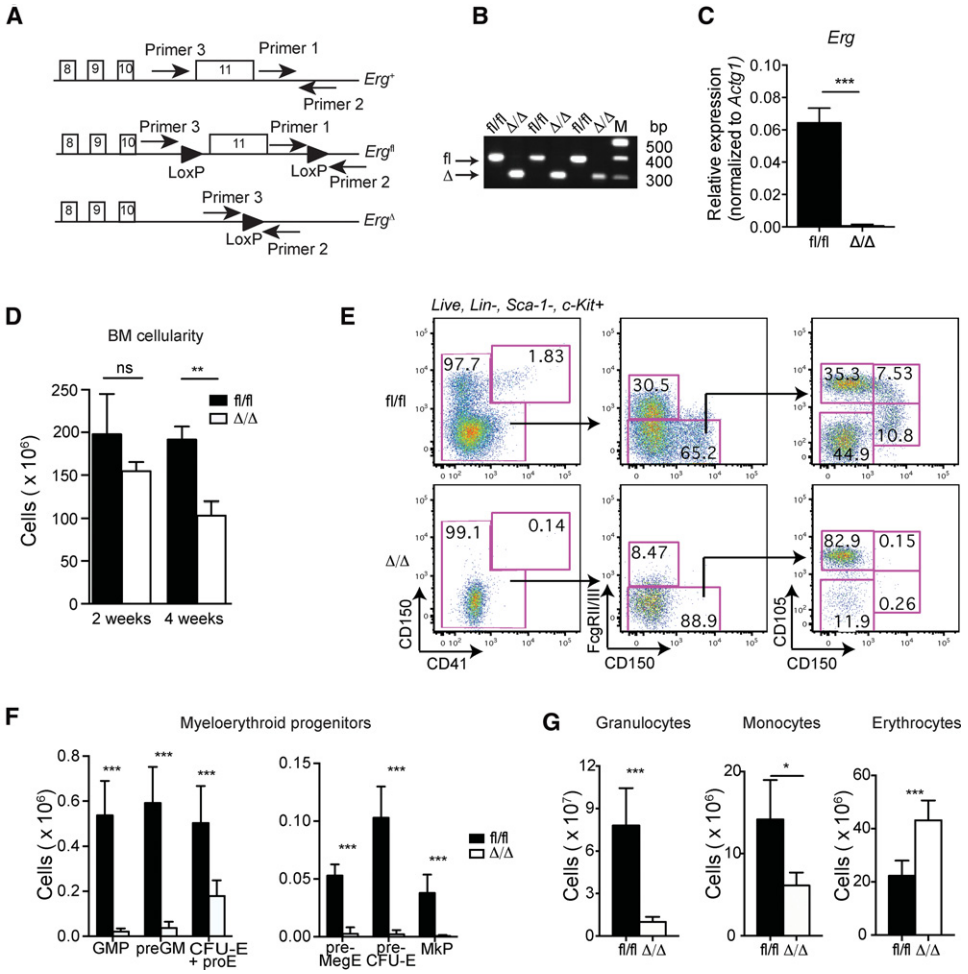

Figure 1. Conditional deletion of *Erg* results in loss of myeloid cells. (*A*) Schematic drawing of the conditional *Erg* knockout mouse model. (*B*) PCR-based genotyping of BM cells derived from pIpC-injected $Erg^{fl/fl}$;±*Mx1Cre* animals illustrating the floxed (fl) and deleted (Δ) *Erg* alleles 2 wk after initiating pIpC injections. We estimate deletion frequencies of >99%. (*C*) The expression of *Erg* mRNA in MPPs derived from $Erg^{fl/fl}$ ($n = 3$) and $Erg^{\Delta/\Delta}$ ($n = 3$) BM 2 wk after initiating pIpC injections. The expression level of the full-length *Erg* transcript is reduced by >100-fold in $Erg^{\Delta/\Delta}$ MPPs. (*D*) BM (2× femur, tibia, and ilium) cell numbers in $Erg^{fl/fl}$ ($n = 6$) and $Erg^{\Delta/\Delta}$ ($n = 6$) mice 2 and 4 wk after pIpC treatment. (*E*) The distribution of myeloid progenitors in $Erg^{fl/fl}$ and $Erg^{\Delta/\Delta}$ mice was analyzed by FACS. (*F*) Quantification of the data in *E*. $Erg^{fl/fl}$, $n = 6$; $Erg^{\Delta/\Delta}$, $n = 7$). (*G*) The distribution of mature myeloid cells in $Erg^{fl/fl}$ ($n = 6$) and $Erg^{\Delta/\Delta}$ ($n = 7$) mice was analyzed by FACS. Data are represented as mean + SD. (*) $P < 0.05$; (**) $P < 0.01$; (***) $P < 0.001$; (ns) not significant. (GMP) Granulocyte–macrophage progenitor; (preGM) pregranulocyte–macrophage; (CFU-E) erythroid colony-forming unit; (pro-E) proerythroblast; (preCFU-E) pre-erythroid colony-forming unit; (preMegE) premegakaryoblast–erythroid progenitor; (MkP) megakaryocyte progenitor. See also Supplemental Figure S1.

monocytic/granulocytic progenitors to be severely reduced 2 wk following deletion of *Erg* (Fig. 1E,F). This translated into a specific depletion of monocytes and granulocytes in both the BM and peripheral blood (PB) (Fig. 1G; Table 1). The reduction of cell numbers was still present at the 4-wk time point, after which partially deleted escaper cells started to repopulate the BM (data not shown).

Erg *is required for HSC activity*

A hypomorphic variant of ERG has previously been shown to impact negatively on key HSC properties. However, the role of ERG within the adult HSC compartment has not been assessed in the context of a complete functional ablation of ERG. We therefore set out to functionally characterize the stem and progenitor (HSC/hematopoietic progenitor cell [HPC]) compartment in our newly developed conditional *Erg* knockout model.

BM analysis 2 wk after complete *Erg* deletion revealed a severe reduction of both immunophenotypic HSCs (Lineage$^-$ Sca-1$^+$ c-Kit$^+$ [LSK] CD150$^+$ CD48$^-$) and MPP cells (LSK CD150$^-$ CD48$^+$) in $Erg^{\Delta/\Delta}$ BM, thus demonstrating an essential role for ERG in HSC maintenance (Fig. 2A, B). This effect was intrinsic to the hematopoietic compartment, as $Erg^{fl/fl}$; *Mx1Cre* recipients transplanted with wild-type BM cells followed by pIpC injection showed no profound hematopoietic defects (Supplemental Fig.

Table 1. *PB counts in* $Erg^{fl/fl}$ *(n = 7) and* $Erg^{\Delta/\Delta}$ *(n = 7) 2 wk after excision of* Erg

	$Erg^{fl/fl}$	$Erg^{\Delta/\Delta}$	*P*-value
Total white blood cells	$5.34 \times 10^6/\mu L \pm 0.95 \times 10^6/\mu L$	$2.76 \times 10^6/\mu L \pm 0.58 \times 10^6/\mu L$	$P < 0.001$
Neutrophils	$0.81 \times 10^6/\mu Ll \pm 0.27 \times 10^6/\mu Ll$	$0.19 \times 10^6/\mu Ll \pm 0.08 \times 10^6/\mu L$	$P < 0.001$
Lymphocytes	$4.07 \times 10^6/\mu L \pm 0.88 \times 10^6/\mu L$	$2.46 \times 10^6/\mu L \pm 0.50 \times 10^6/\mu L$	$P < 0.01$
Monocytes	$0.18 \times 10^6/\mu L \pm 0.05 \times 10^6/\mu L$	$0.01 \times 10^6/\mu L \pm 0.01 \times 10^6/\mu L$	$P < 0.001$
Red blood cells	$8.27 \times 10^9/\mu L \pm 0.41 \times 10^9/\mu L$	$8.89 \times 10^9/\mu L \pm 0.50 \times 10^9/\mu L$	$P < 0.05$
Hemoglobin	7.14 µmol/µL ± 0.43 µmol/µL	7.76 µmol/µL ± 0.34 µmol/µL	$P < 0.05$
Platelets	$1261 \times 10^6/\mu L \pm 379 \times 10^6/\mu L$	$405 \times 10^6/\mu L \pm 270 \times 10^6/\mu L$	$P < 0.001$

Data are represented as mean ± SD.

S1B). In contrast, wild-type recipients (CD45.1) transplanted with $Erg^{fl/fl}$; *Mx1Cre* (CD45.2) and wild-type (CD45.1) BM in a 10:1 ratio and subsequently subjected to ERG ablation showed a marked reduction of donor-derived CD45.2 cells in the PB (Fig. 2C) and were essentially devoid of CD45.2 HSCs/HPCs at the 20-wk experimental end point (Fig. 2D; Supplemental Fig. S2A). These findings clearly demonstrate the marked functional impairment of $Erg^{\Delta/\Delta}$ HSCs during steady-state hematopoiesis.

To assess the ability of *Erg*-deficient BM cells to reconstitute the hematopoietic system, we next competitively transplanted CD45.2 BM ($Erg^{\Delta/\Delta}$ or $Erg^{fl/fl}$) donor cells and CD45.1 wild-type competitor cells in different ratios. Here we found that $Erg^{\Delta/\Delta}$ BM cells were essentially unable to contribute to hematopoietic reconstitution when transplanted in equal (1:1) ratios and only contributed marginally when transplanted in 10-fold excess (Fig. 2E, F). To assess this at the level of individual HSC and MPP populations, we subsequently transplanted 30 purified HSCs (LSK, $CD150^+$) or 150 purified MPPs (LSK, $CD150^-$) from $Erg^{\Delta/\Delta}$ or $Erg^{fl/fl}$ BM along with 2×10^5 unfractionated support cells. In accordance with our previous findings, $Erg^{\Delta/\Delta}$ HSCs were unable to contribute to hematopoietic reconstitution (Fig. 2G). In contrast, we observed a marginal, albeit significant, contribution from $Erg^{\Delta/\Delta}$ MPPs 3 wk after transplantion, suggesting that ERG is mainly important for truly reconstituting HSCs and less so for their downstream progeny (Fig. 2H). Collectively, these findings demonstrate that ERG is indispensable for long-term hematopoietic reconstitution.

Next, we assessed whether the gene dosage of *Erg* had an impact on hematopoiesis and, in particular, HSC function, as suggested by the previous analysis of the hypomorphic $Erg^{Mid2/+}$ variant (Supplemental Fig. S3A,B). Indeed, we found that adult $Erg^{+/-}$ mice displayed similar, albeit less pronounced, reductions in hematopoietic populations, including myeloid progenitors (Supplemental Fig. S3C,D) as well as immunophenotypic HSCs and MPPs (Supplemental Fig. S3E,F). Importantly, we also found $Erg^{+/-}$ BM cells to be highly impaired in hematopoietic reconstitution, demonstrating that even a moderate lowering of ERG levels has a strong impact on HSC function (Supplemental Fig. S3G).

Finally, given the pronounced HSC phenotype in $Erg^{\Delta/\Delta}$ BM, we reasoned that pIpC-treated $Erg^{fl/fl}$; *Mx1Cre* animals could be transplanted without prior conditioning. Indeed, when transplanted in the absence of irradiation, we found that these animals were almost completely reconstituted by wild-type BM, whereas wild-type BM failed to engraft in $Erg^{fl/fl}$ recipients under the same conditions (Fig. 2I; Supplemental Fig. S2B). These data suggest that the $Erg^{fl/fl}$; *Mx1Cre* model might serve as a useful tool in BM transplantation assays when conditioning by irradiation or drugs is not appropriate. In summary, loss of *Erg* has dramatic effects on both the numbers and the ability of HSCs to reconstitute the hematopoietic system, and, collectively, our functional analyses demonstrate that ERG is indispensable for HSC maintenance and self-renewal.

HSC migration, homing, and adhesion are not dependent on ERG activity

Having demonstrated the unique importance of ERG for HSC function, we next set out to identify which key properties were affected by its loss. The rapid and massive reduction in $Erg^{\Delta/\Delta}$ HSCs could in principle be explained by HSC egress from the BM to the PB and/or other hematopoietic organs. To test this, we quantified the numbers of HSCs ($CD45^+$ $EPCR^+$ $CD150^+$ $CD48^-$; to exclude confounding issues of pIpC-induced deregulation of Sca-1 expression) (Essers et al. 2009) in the PB and spleen at early time points after *Erg* deletion but found no evidence for increased numbers of HSCs in $Erg^{\Delta/\Delta}$ animals (Fig. 3A,B). In contrast, we found a marked reduction in the colony-forming potential of $Erg^{\Delta/\Delta}$ splenocytes (Fig. 3C), further demonstrating that increased HSC egress from the BM is unlikely to explain the strong phenotype in *Erg*-deficient animals.

Because impaired homing capacity could also potentially affect the numbers and function of HSCs in $Erg^{\Delta/\Delta}$ and $Erg^{+/-}$ BMs, we tested the ability of carboxyfluorescein succinimidyl ester (CFSE)-labeled c-Kit^+ $Erg^{\Delta/\Delta}$ progenitors as well as sorted $Erg^{+/-}$ HSCs to home to the BM following transplantation. However, we did not observe any marked differences in the number of labeled cells in the recipient BM in any of these assays, suggesting that at least $Erg^{\Delta/\Delta}$ HPCs and $Erg^{+/-}$ HSCs can home efficiently to their BM niches in the absence of ERG (Fig. 3D,E).

Finally, we investigated the ability of $Erg^{+/+}$ and $Erg^{+/-}$ HSCs to adhere to stroma cells in vitro. In support of our previous analyses, $Erg^{+/-}$ and $Erg^{+/+}$ HSCs had comparable capacities to adhere to stroma cells (Fig. 3F). Thus, in conclusion, our data do not support a major role for ERG in HSC trafficking, homing, or adhesion.

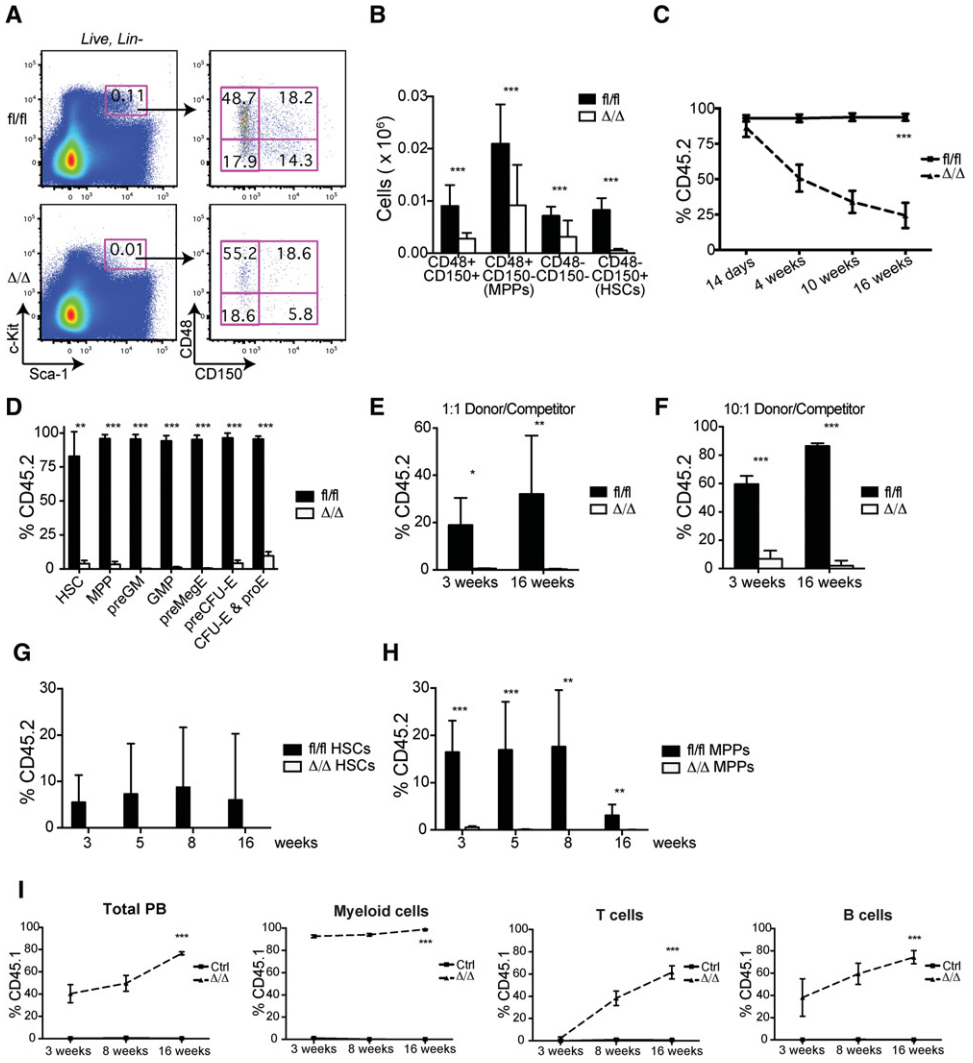

Figure 2. ERG maintains HSC numbers and function. (*A*) FACS analysis showing the distribution of stem and progenitor cells in $Erg^{fl/fl}$ and $Erg^{\Delta/\Delta}$ mice 2 wk after *Erg* deletion. (*B*) Quantification of the data in *A*: Total numbers of stem and progenitor cells per 2× femur, tibia, and ilium. $Erg^{fl/fl}$, $n = 6$; $Erg^{\Delta/\Delta}$, $n = 7$. (*C*) Analysis of donor cell contribution to the PB from CD45.1 recipients transplanted with $Erg^{fl/fl}$ or $Erg^{fl/fl}$; *Mx1Cre* BM (CD45.2) in a 10:1 ratio with competitor BM. The recipient mice were treated with pIpC following transplantation to induce *Erg* deletion in the donor cell compartment. The indicated time is relative to *Erg* deletion. $Erg^{fl/fl}$, $n = 9$; $Erg^{\Delta/\Delta}$, $n = 12$. (*D*) Analysis of BM from mice in *C* at 20 wk after deletion of *Erg*. $Erg^{fl/fl}$, $n = 3$; $Erg^{\Delta/\Delta}$, $n = 3$. (*E*) Analysis of PB from CD45.1 recipients transplanted with $Erg^{fl/fl}$ ($n = 6$) or $Erg^{\Delta/\Delta}$ ($n = 6$) BM (CD45.2) in a 1:1 ratio with competitor BM (CD45.1). (*F*) As in *E* but using a 10:1 donor:competitor ratio. (*G*) Analysis of donor cell contributions to PB from CD45.1 recipients competitively transplanted with 30 $Erg^{fl/fl}$ ($n = 13$) or $Erg^{\Delta/\Delta}$ ($n = 2$) HSCs (CD45.2). (*H*) Analysis of donor cell reconstitution in PB from CD45.1 recipients competitively transplanted with 150 $Erg^{fl/fl}$ ($n = 7$) or $Erg^{\Delta/\Delta}$ ($n = 8$) MPPs (CD45.2). (*I*) Analysis of PB from $Erg^{fl/fl}$ ($n = 5$; pIpC injected), $Erg^{fl/fl}$; *Mx1Cre* ($n = 2$; not injected with pIpC), and $Erg^{\Delta/\Delta}$ ($n = 4$; pIpC injected) mice transplanted with wild-type CD45.1 BM. Ctrl represents pooled data from $Erg^{fl/fl}$ and $Erg^{fl/fl}$; *Mx1Cre*. Data are represented as mean + SD. (*) $P < 0.05$; (**) $P < 0.01$; (***) $P < 0.001$. See also Supplemental Figures S2 and S3.

ERG maintains quiescence and prevents differentiation of HSCs

Our phenotypic analyses of the HSC compartment demonstrate that ERG is indispensable for HSC maintenance. This was corroborated further by in vitro long-term culture-initiating cell (LTC-IC) assays (a surrogate self-renewal assay) in which the ability of $Erg^{\Delta/\Delta}$ HSCs to form colonies was reduced by 80% (Fig. 4A). To determine whether this reduction was caused by alterations in proliferation, we single-sorted $Erg^{fl/fl}$; *R26-CreER* HSCs and assessed their potential for proliferation in vitro following the deletion of *Erg* by 4-hydroxytamoxifen (4-OHT). However, no differences were observed between control and knockout HSCs in terms of either plating efficiency or their ability to divide (Fig. 4B). Consistent with the in vitro data, cell cycle analyses of freshly isolated $Erg^{+/-}$ and $Erg^{+/+}$ HSCs demonstrated similar amounts of cells in the $S/G_2/M$ phases, suggesting that ERG does not affect the proliferative capacity of HSCs per se (Fig. 4D,E).

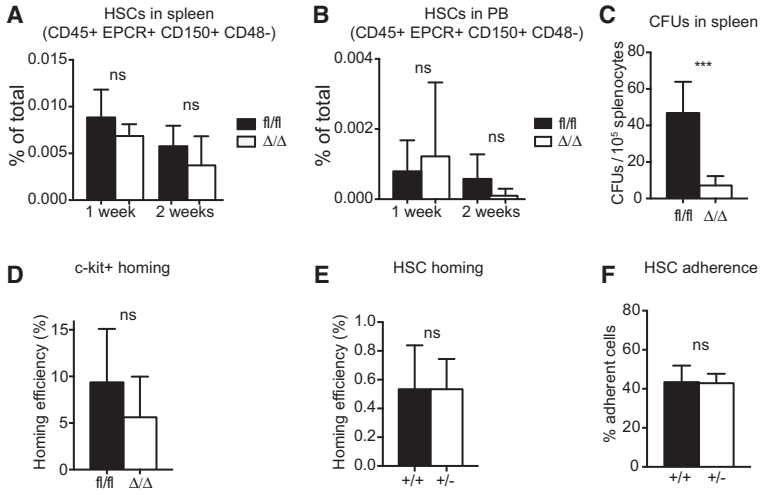

Figure 3. The impact of ERG on HSC localization, migration, and adhesion properties. (*A*) FACS analysis was used to determine HSC (Lineage$^-$ EPCR$^+$ CD45$^+$ CD150$^+$ CD48$^-$) numbers in the spleens of $Erg^{fl/fl}$ (n = 3–4) and $Erg^{\Delta/\Delta}$ (n = 2–5) mice 1 and 2 wk after *Erg* deletion. (*B*) FACS analysis was used to determine HSC (Lineage$^-$ EPCR$^+$ CD45$^+$ CD150$^+$ CD48$^-$) numbers in the PB of $Erg^{fl/fl}$ (n = 4–7) and $Erg^{\Delta/\Delta}$ (n = 4–6) mice 1 and 2 wk after *Erg* deletion. (*C*) CFUs in M3434 semisolid medium of splenocytes from $Erg^{fl/fl}$ (n = 6) and $Erg^{\Delta/\Delta}$ (n = 6) mice. (*D*) Homing analysis of $Erg^{fl/fl}$ (n = 13) and $Erg^{\Delta/\Delta}$ (n = 11) c-Kit$^+$ BM cells 3 h after intravenous injection of 10,000 carboxyfluorescein succinimidyl ester (CFSE)-labeled cells per irradiated recipient. (*E*) Homing analysis of $Erg^{+/+}$ (n = 5) and $Erg^{+/-}$ (n = 5) HSCs (LSK CD150$^+$ CD48$^-$) 12 h after intravenous injection of 3000 CFSE-labeled HSCs per irradiated recipient. (*F*) In vitro adhesion of $Erg^{+/+}$ (n = 10) and $Erg^{+/-}$ (n = 9) GFP$^+$ HSCs (LSK CD150$^+$ CD48$^-$) to FBMD-1stromal cells following a180° flip. Data are represented as mean + SD. (ns) Not significant; (***) $P < 0.001$. See also Supplemental Figure S3.

However, we did observe a marked decrease in the amount of quiescent (G_0) HSCs and a compensatory increase of cells in G_1, suggesting that ERG is important for maintaining HSCs in quiescence. As this increase is comparable with what is observed in other mouse lines exhibiting far less dramatic HSC phenotypes (e.g., *Cebpa*-deficient HSCs), we consider it unlikely that this is responsible for the complete loss of HSCs observed upon ERG ablation (Hasemann et al. 2014). Significantly, other cellular properties associated with reduced HSC maintenance, such as accumulation of reactive oxygen species (ROS) and cell death, were also not different between $Erg^{+/-}$ and $Erg^{+/+}$ HSCs (Fig. 4C,D,F).

Exit from quiescence is presumably one of the first steps when HSCs commit to differentiation, and we reasoned that loss of *Erg* could potentially increase the propensity of HSCs to differentiate, which in turn could explain the dramatic drop in HSC numbers that we observed. As a first step to test this hypothesis, we assessed the myeloid differentiation potential of FACS-sorted HSCs, MPPs, pregranulocyte/macrophages (preGMs) and granulocyte/macrophage progenitors (GMPs) and found that loss of *Erg* was entirely compatible with normal myeloid differentiation (Fig. 4G,H). Next, we rationalized that if $Erg^{\Delta/\Delta}$ HSCs were lost through increased differentiation, this should initially be discernable in the HSC compartment before becoming apparent in the downstream MPP populations. Interestingly, we saw a dramatic decrease in the HSC/MPP ratio 2 wk following deletion of *Erg*, which was normalized 2 wk later (Fig. 4I). We next subjected these data to mathematical modeling (see the Supplemental Material). Significantly, the model that best fits the experimental data displays a 25-fold increase in the relative differentiation rate of $Erg^{\Delta/\Delta}$ HSCs (Fig. 4J; Supplemental Fig. S4). Importantly, the increased differentiation rate in $Erg^{\Delta/\Delta}$ HSCs is very robust and only varies between 17-fold and 34-fold when the relative proliferation rate of $Erg^{\Delta/\Delta}$ to wild-type HSCs is changed from 0.5 to 2.0, thereby demonstrating a remarkable stability of the model over a range of relative proliferation rates (Fig. 4K). In conclusion, both the experimental data and our mathematical modeling are consistent with a role for ERG in restricting HSC differentiation.

ERG regulates stem cell genes directly

To identify the molecular mechanisms underlying the function of ERG in HSCs, we performed gene expression analysis in $Erg^{+/-}$ and $Erg^{+/+}$ HSCs (LSK CD150$^+$ CD48$^-$). We identified 179 and 174 genes that were down-regulated and up-regulated, respectively, by at least 1.5-fold in $Erg^{+/-}$ HSCs compared with controls (Supplemental Table S1), and several of the genes, such as *Cxcl12*, are known to play a role in HSC biology. Supporting an important role of ERG in HSC maintenance, gene set enrichment analysis (GSEA) demonstrated down-regulation of stem cell signatures (NG_STEM and NG_S.MPP) in $Erg^{+/-}$ HSCs. Similarly, a signature associated with lymphoid–myeloid priming of HSCs (NG_S.MYLY) is also down-regulated in $Erg^{+/-}$ HSCs, whereas a signature associated with erythroid differentiation is up-regulated (MANSSON_E), in line with the relative mild erythroid phenotypes in $Erg^{+/-}$ animals (Fig. 5A; Supplemental Fig. S3). Consistent with the analysis of $Erg^{+/-}$ versus $Erg^{+/+}$ HSCs, further gene expression analyses in $Erg^{\Delta/\Delta}$ versus $Erg^{fl/fl}$ MPPs demonstrated that loss of *Erg* in the MPP compartment also correlated negatively with HSC gene signatures and positively with an erythroid gene signature (Fig. 5B; Supplemental Table S2). Finally, we note that a signature representing MYC downstream targets is selectively up-regulated in $Erg^{+/-}$ HSCs (Fig. 5C).

In order to identify direct ERG target genes, we next compared the $Erg^{+/-}$ and $Erg^{+/+}$ HSC gene expression data set with published ERG ChIP-seq (chromatin immunoprecipitation [ChIP] combined with deep sequencing) data from the HPC-7 progenitor cell line (Wilson et al. 2010). Sixty-two percent of the down-regulated genes (Supplemental Table S3) and 56% of the up-regulated

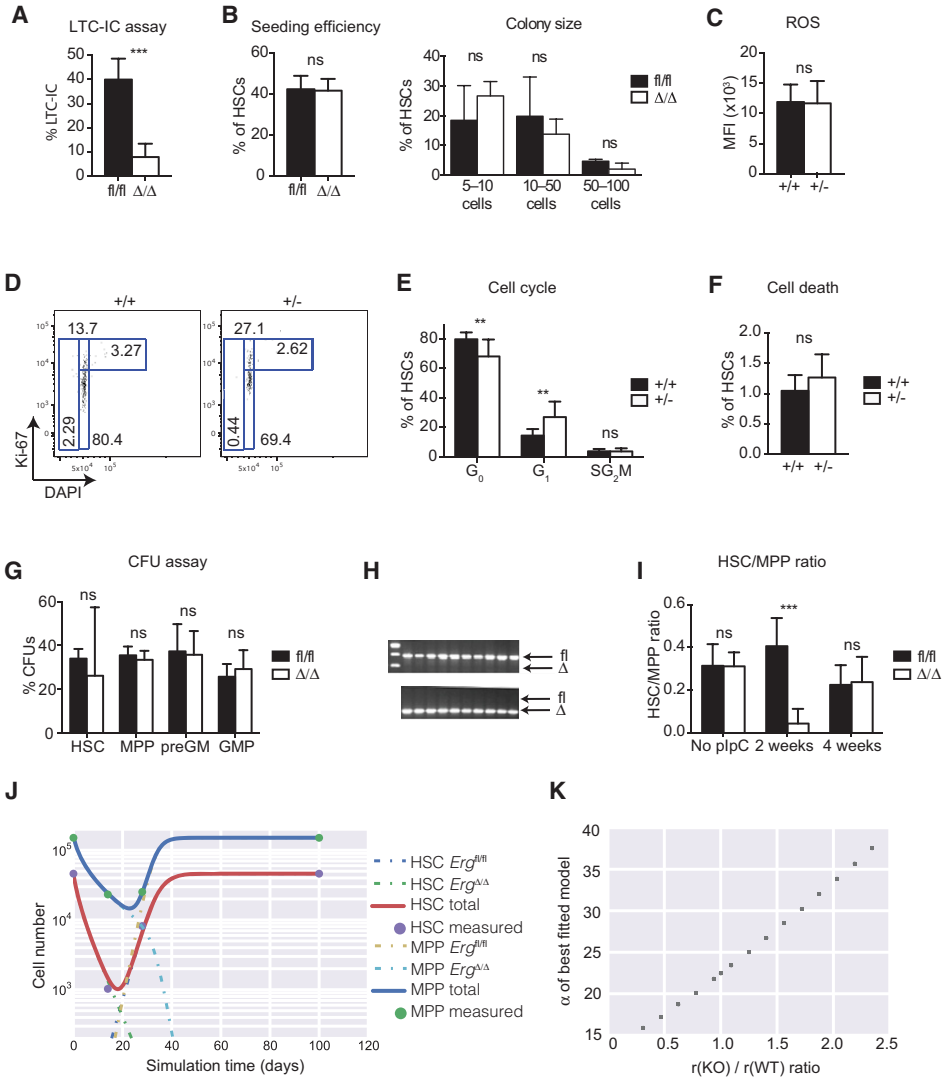

Figure 4. Loss of *Erg* results in differentiation of the HSCs. (*A*) LTC-IC assay of sorted $Erg^{fl/fl}$ ($n = 220$ HSCs from four mice) and $Erg^{\Delta/\Delta}$ ($n = 168$ HSCs from six mice) HSCs (Lineage$^-$ EPCR$^+$ CD45$^+$ CD150$^+$ CD48$^-$). Sorted HSCs were cultured on FBMD-1 stromal cells for 5 wk, and LTC-IC capacity was evaluated by counting colonies arising after an additional week of culture in semisolid M3434 medium. (*B*) Colony-forming ability (seeding efficiency [*left* panel] and colony size [*right* panel]) of single-sorted, in vitro excised $Erg^{fl/fl}$ ($n = 330$ HSCs from five mice) and $Erg^{\Delta/\Delta}$ ($n = 330$ HSCs from six mice) HSCs (LSK CD150$^+$ CD48$^-$) cultured in SFEM supplemented with cytokines for 8 d. (*C*) ROS levels in $Erg^{+/+}$ ($n = 4$) and $Erg^{+/-}$ ($n = 4$) HSCs were measured by CM-H2DCFDA staining followed by FACS analysis. (MFI) Mean fluorescence intensity. (*D*) FACS analysis of cells stained with Ki67 and DAPI to analyze cell cycle distribution and cell death in $Erg^{+/+}$ ($n = 10$) and $Erg^{+/-}$ ($n = 13$) HSCs. (*E*) Quantification of the cell cycle data in *D*. (*F*) Quantification of the cell death data in *D*. (*G*) CFU assays (in M3434 semisolid medium) of sorted stem and progenitor cells from $Erg^{fl/fl}$ (HSCs, $n = 6$; MPPs, $n = 2$; preGMs, $n = 6$; GMPs, $n = 2$), and $Erg^{\Delta/\Delta}$ (HSCs, $n = 8$; MPPs, $n = 2$; preGMs, $n = 8$; GMPs, $n = 2$). (*H*) Genotyping of colonies from CFU assays in *G*. (*Top* gel) $Erg^{fl/fl}$. (*Bottom* gel) $Erg^{\Delta/\Delta}$. (*I*) Numbers of HSCs and MPPs at different time points after pIpC injection were determined by FACS analysis. The graph illustrates HSC/MPP ratios at different time points after pIpC injections in $Erg^{fl/fl}$ (No pIpC, $n = 4$; 2 wk, $n = 6$; 4 wk, $n = 7$) and $Erg^{\Delta/\Delta}$ (No pIpC, $n = 3$; 2 wk, $n = 7$; 4 wk, $n = 5$) BM. (*J*) Mathematical modeling of the data in *I* showing the changes in HSC and MPP numbers in $Erg^{\Delta/\Delta}$ BM. Please note that the model takes into account that the deletion is <100%, leading to the emergence of escaper cells (HSC $Erg^{fl/fl}$ and MPP $Erg^{fl/fl}$). The experimental data are depicted by circles. (*K*) α of the relative differentiation rates of knockout/wild-type HSCs of the best-fitted model, plotted as a function of the relative proliferation rates of knockout/wild-type HSCs. See the Supplemental Material for further details of the analyses. Data are represented as mean + SD. (**) $P < 0.01$; (***) $P < 0.001$; (ns) not significant. See also Supplemental Figure S4.

genes (Supplemental Table S4) were bound by ERG within 800 base pairs (bp) of their transcriptional start sites (TSSs), which is significantly more than randomly chosen nonregulated genes (38%, $P = 0.0476$ for up-regulated genes; $P = 3 \times 10^{-4}$ for down-regulated genes, in a permutation test drawing from genes with annotated TSSs) (Fig. 5D). Interestingly, gene ontology analysis of the ERG-bound down-regulated genes identified several HSC gene

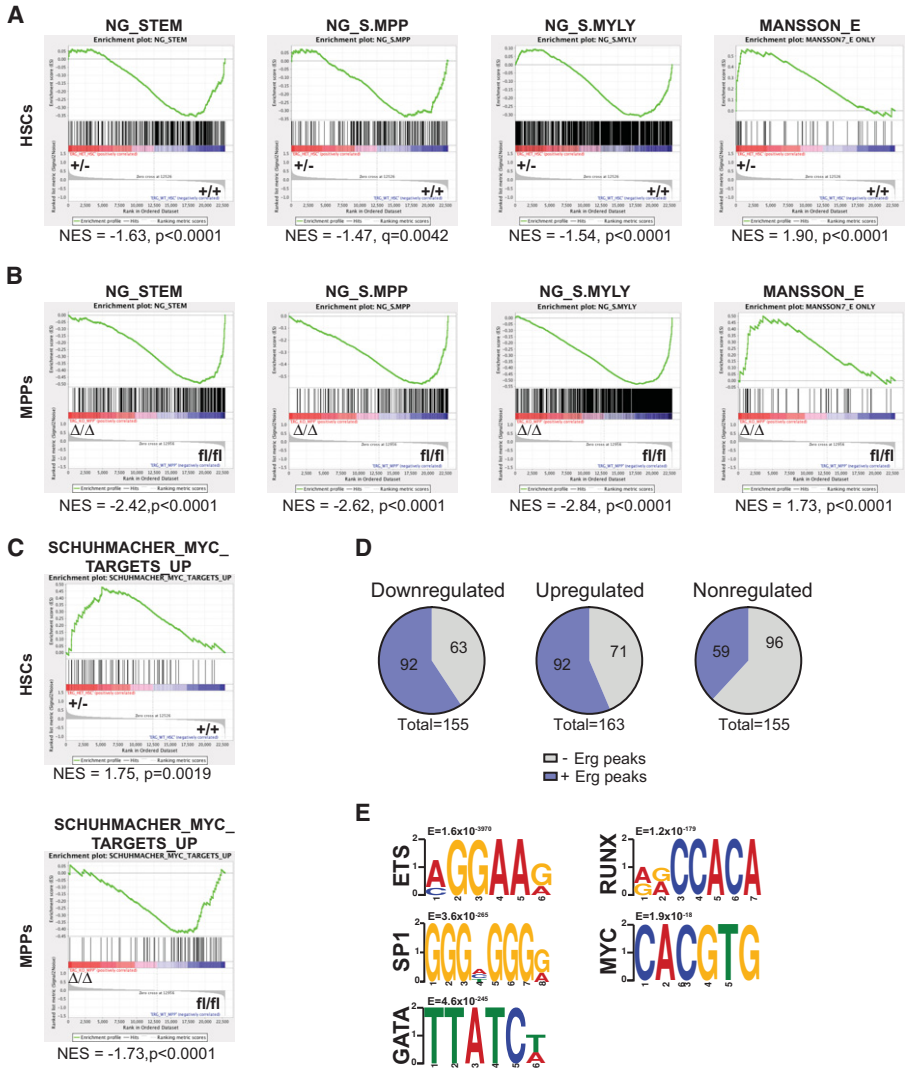

Figure 5. ERG regulates distinct transcriptional programs in HSCs (*A*) HSCs (LSK CD150$^+$ CD48$^-$) were sorted from *Erg*$^{+/-}$ and *Erg*$^{+/+}$ mice for microarray analysis, and the resulting gene expression data were used for GSEA using selected hematopoietic signatures. (*B*) GSEA of *Erg*$^{\Delta/\Delta}$ versus *Erg*$^{fl/fl}$ MPPs using selected hematopoietic signatures. (*C*) GSEA illustrating the selective up-regulation of MYC target genes in *Erg*$^{+/-}$ HSCs. (*D*) Binding of ERG to transcription start sites (TSSs; ±800 base pairs [bp]) of genes that are down-regulated, up-regulated, or nonregulated in *Erg*$^{+/-}$ versus *Erg*$^{+/+}$ HSCs. ChIP-seq (chromatin immunoprecipitation [ChIP] combined with deep sequencing) data originate from HPC-7 cells (Wilson et al. 2010). (*E*) DREME motif analysis identifying transcription factor-binding sites enriched near ERG-bound regions.

sets (Supplemental Table S5), suggesting that ERG activates the expression of a group of genes important for HSC function by direct binding to their promoters. Moreover, in line with the GSEA data above, gene ontology analysis of the ERG-bound up-regulated genes identified several MYC target gene sets (Supplemental Table S6), suggesting that ERG might functionally repress the expression of MYC downstream targets in HSCs. This is further supported by motif analysis that, besides identifying the ERG consensus motif and motifs bound by already known coregulators such as RUNX and GATA factors, also identifies the MYC consensus motif in ERG-bound regions (Fig. 5E; Supplemental Table S7). Further analysis of the ERG-bound genes revealed that genes down-regulated upon *Erg* deletion were enriched for GATA/RUNX motifs in their promoters and frequently constituted genes involved in stem cell function (Supplemental Tables S8, S9). In contrast, ERG-bound genes that were up-regulated upon *Erg* deletion had increased occurrences of GATA/MYC motifs in their promoters and preferentially constituted MYC target genes. The latter finding is consistent with a model in which ERG represses the expression of MYC target genes by direct binding to their promoters.

Collectively, our bioinformatics analyses suggest that ERG functions as both a transcriptional activator and a repressor in HSCs and coordinately regulates the expression of genes associated with self-renewal and differentiation.

ERG controls MYC-dependent differentiation in HSCs

Our data are compatible with a model in which the main function of ERG is to restrict HSC differentiation, and this potentially could be mediated through repression of a MYC-dependent transcriptional program in HSCs. In other words, loss of *Erg* would phenotypically mimic overexpression of *Myc*, which is associated with increased HSC differentiation (Wilson et al. 2004). Chemicals targeting the bromodomain and extraterminal (BET) family of proteins such as CPI-203 and JQ-1 are known inhibitors of *Myc* mRNA expression and act through interfering with a superenhancer that controls *Myc* expression (King et al. 2013; Loven et al. 2013). Thus, to substantiate our model, we tested whether CPI-203 could rescue the *Erg*-deficient HSC phenotype.

We first confirmed the activity of this compound in HSCs by culturing sorted LSK CD150$^+$ CD48$^-$ cells from *Erg*$^{+/-}$ and *Erg*$^{+/+}$ mice in the presence of 0.5 μM CPI-203 for 24 h. As expected, *Myc* mRNA was reduced by twofold to threefold compared with mock-treated HSCs in both groups, while there was no difference in *Myc* expression between the *Erg*$^{+/-}$ and *Erg*$^{+/+}$ groups (Fig. 6A). We next treated *Erg*$^{fl/fl}$ and *Erg*$^{fl/fl}$; *Mx1Cre* mice with CPI-203 simultaneously with *Erg* deletion through pIpC injection (Fig. 6B). Strikingly, CPI-203 restored the numbers of immunophenotypic HSCs (defined as c-Kit$^+$ EPCR$^+$ CD150$^+$ CD48$^-$, since Sca-1 expression is not reliable shortly after pIpC administration) to normal levels in *Erg*$^{\Delta/\Delta}$ BM while increasing HSC numbers in *Erg*$^{fl/fl}$ controls (Fig. 6C). Similarly, CPI-203 rescued the numbers of immunophenotypic *Erg*$^{+/-}$ HSCs (LSK CD150$^+$ CD48$^-$) to normal levels and again increased HSC numbers in control animals (Fig. 6D,E). These experiments clearly demonstrate that a reduction of MYC activity can indeed rescue the effect of *Erg* deletion on HSC numbers, likely through an anti-differentiation mode of action. Although HSCs are increased above normal levels upon *Myc* down-regulation in *Erg*$^{+/+}$ mice, it is interesting to note that the extent of this increase is larger in *Erg*$^{+/-}$ mice (2.3-fold) than in the *Erg*$^{+/+}$ controls (1.5-fold) (Fig. 6E). In addition, there seems to be a particularly enhancing effect of CPI-203 on the proportion of CD150$^+$ CD48$^-$ cells within the LSK population in *Erg*$^{+/-}$ mice compared with controls (Fig. 6F), pointing toward an exclusively restoring effect of *Myc* down-regulation in the differentiation-prone *Erg*-deficient HSCs.

To test whether *Myc* inhibition would have a similar rescuing effect on HSC function as well, we transplanted BM cells from CPI-203-treated *Erg*$^{+/-}$ and *Erg*$^{+/+}$ mice into lethally irradiated mice along with unmanipulated BM competitor cells (Fig. 6D). CPI-203 slightly but significantly improves the multilineage engraftment capacity of *Erg*$^{+/-}$ HSCs compared with mock treatment, demonstrating that *Myc* down-regulation partly restores HSC function (Fig. 6G,H). Consistent with its effect on the numbers of immunophenotypic HSCs, *Myc* down-regulation also increases the engraftment of *Erg*$^{+/+}$ cells. Chimerism within the HSC compartment 20 wk after transplantation did not vary significantly between the CPI-203-treated and mock-treated groups irrespective of genotype (Fig. 6I). This is an anticipated result given that CPI-203 is not administered to the recipients and further verifies the anti-differentiating effect of this drug rather than having effects on other HSC-promoting properties like self-renewal or survival. Such effects would be expected to read out as increased long-term repopulation capacity of the HSC pool. The transplantation experiments therefore confirm that a short period of *Myc* inhibition in *Erg*-deficient donor mice is able to prevent differentiation of HSCs and thereby partly rescue the numbers of multilineage reconstituting HSCs.

Finally, we wanted to test whether *Myc* down-regulation leads to normalization of genes otherwise up-regulated in the *Erg*-deficient setting. For this, we selected top-scoring genes from the MYC target gene set that were found to be up-regulated upon *Erg* loss (Supplemental Table S6) and performed qRT–PCR analysis on *Erg*$^{+/-}$ and *Erg*$^{+/+}$ c-Kit$^+$ cells treated with CPI-203 for 24 h in vitro. We verified the up-regulated expression of several MYC target genes in *Erg*$^{+/-}$ cells (*Dkc1*, *Ccnb1*, *Cks2*, *Tfrc*, and *Pigp*), while *Myc* mRNA itself was unchanged, consistent with our gene expression analysis (Fig. 6J). Moreover, a subset of the tested MYC target genes was down-regulated in both *Erg*$^{+/-}$ and *Erg*$^{+/+}$ c-Kit$^+$ cells following CPI-203 treatment in vitro (*Dkc1*, *Ccnb1*, and *Pold2*), indicating that these genes are indeed direct targets of MYC and that *Erg* status can influence their expression levels. Other tested genes were increased in *Erg*$^{+/-}$ cells compared with control but were not obviously sensitive to CPI-203 treatment (*Cks2*, *Tfrc*, and *Pigp*) and may therefore not be coregulated by ERG/MYC in this setting (Fig. 6J). Collectively, these data support a model in which ERG regulates the balance between HSC self-renewal and differentiation through repression of MYC target genes and activation of self-renewal genes (Fig. 6K).

ERG is dispensable for leukemic transformation

It is well established that ERG overexpression or ERG-containing fusion proteins are drivers of malignant transformation in leukemia and solid tumors and that in vitro depletion of ERG in these cases can attenuate cell growth (Marcucci et al. 2005, 2007; Baldus et al. 2006; Salek-Ardakani et al. 2009; Tsuzuki et al. 2011; Carmichael et al. 2012; Rosen et al. 2012). However, the extent to which the presence of ERG is a general requirement for tumor initiation and maintenance has not been addressed. To address this important issue, we crossed the *Erg*^{fl} allele into well-established models of murine T-ALL and AML. Initially, we generated *Erg*$^{fl/fl}$; *CD2iCre* animals in which the expression of CRE initiates in common lymphoid progenitors (CLPs), resulting in a pan-lymphoid deletion of *Erg*. BM cells from these animals and *Erg*$^{fl/fl}$ controls were then transduced with retrovira expressing either *NOTCH-ICD* or *Nras*^{G12D} and subsequently transplanted into lethally irradiated recipients. These mice developed short latency T-ALLs with accumulation of mainly CD4$^+$CD8$^+$ or CD4^{low}CD8$^+$ leukemic cells in hematopoietic organs (Fig. 7A–C). Although the *Erg*-

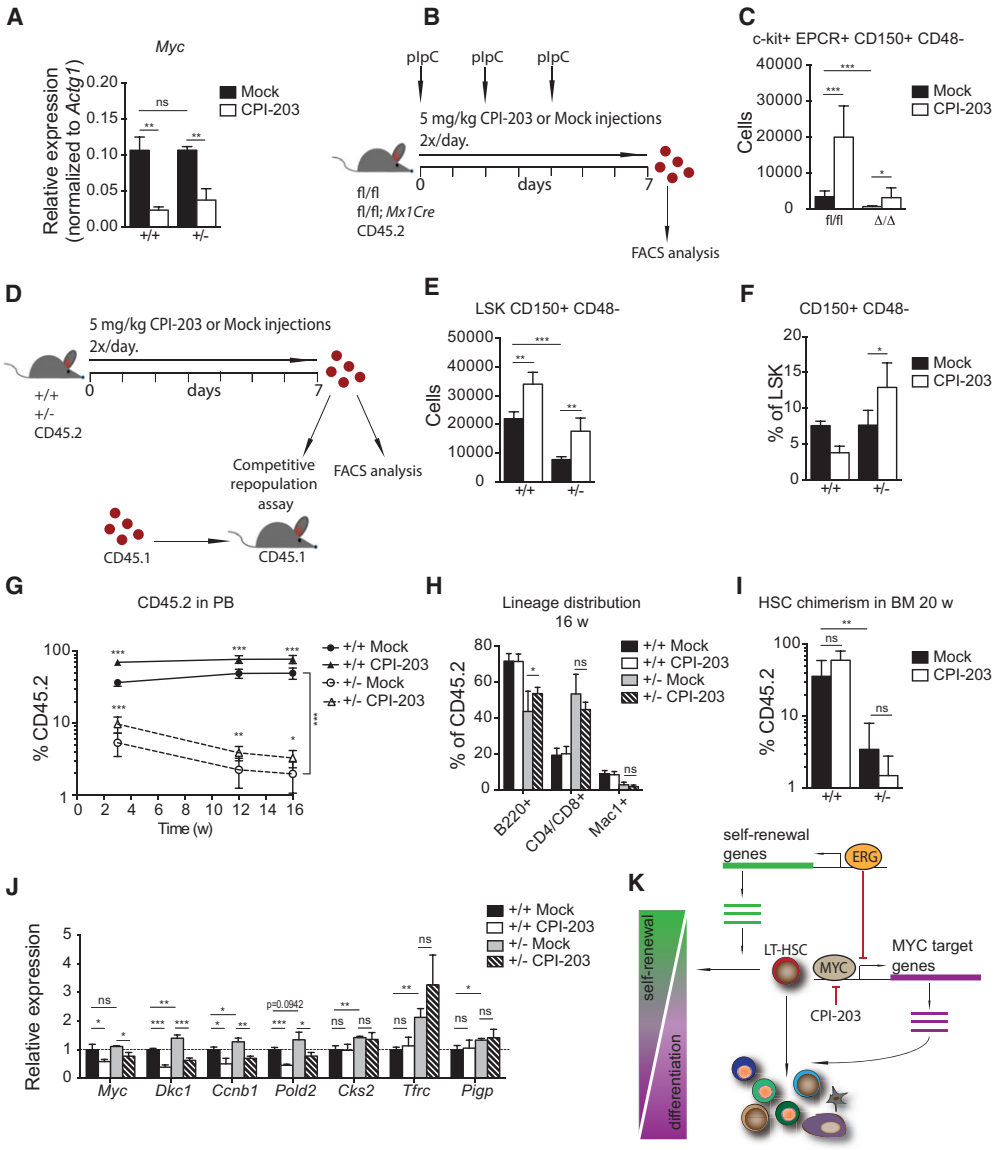

Figure 6. The HSC maintenance defect in *Erg*-deficient mice can be rescued by modulation of *Myc* activity. (*A*) qRT–PCR analysis of *Myc* mRNA expression in LSK CD150$^+$ CD48$^-$ HSCs from *Erg*$^{+/+}$ ($n = 3$) and *Erg*$^{+/-}$ ($n = 3$) mice following 24 h of treatment with CPI-203 in vitro. (*B*) Schematic overview of pIpC and CPI-203 administration in *Erg*$^{fl/fl}$ and *Erg*$^{fl/fl}$; *Mx1Cre* mice. (*C*) FACS analysis was used to determine total numbers of Lin$^-$ c-Kit$^+$ EPCR$^+$ CD150$^+$ CD48$^-$ HSCs in 2× femur, tibia, and ilium of *Erg*$^{fl/fl}$ and *Erg*$^{\Delta/\Delta}$ mice ($n = 7$–10) after 1 wk of CPI-203 treatment. (*D*) Schematic overview of CPI-203 administration and analyses performed in *Erg*$^{+/+}$ and *Erg*$^{+/-}$ mice. (*E*) FACS analysis was used to determine total numbers of LSK CD150$^+$ CD48$^-$ HSCs in 2× femur, tibia, and ilium of *Erg*$^{+/+}$ ($n = 3$–4) and *Erg*$^{+/-}$ mice ($n = 4$) following 1 wk of CPI-203 treatment. (*F*) The percentage of CD150$^+$ CD48$^-$ cells within the LSK compartment in *Erg*$^{+/+}$ ($n = 3$–4) and *Erg*$^{+/-}$ ($n = 4$) mice following 1 wk of CPI-203 treatment. (*G*) BM cells from CPI-203-treated *Erg*$^{+/+}$ ($n = 3$–4) and *Erg*$^{+/-}$ ($n = 4$) mice were used as input for the competitive repopulation assay, and contributions to the PB were measured in recipients ($n = 7$–12) at 3, 12, and 16 wk after transplantation. (*H*) Distribution of B cells, T cells, and myeloid cells within the donor cell compartment in PB 16 wk after transplantation. (*I*) Donor cell chimerism within the LSK CD150$^+$ CD48$^-$ HSC compartment in BM 20 wk after transplantation. (*J*) qRT–PCR analysis of *Myc* and MYC target gene mRNA expression in c-Kit$^+$ cells from *Erg*$^{+/+}$ ($n = 3$) and *Erg*$^{+/-}$ ($n = 3$) mice following 24 h of treatment with CPI-203 in vitro. Gene expression is normalized to *Actg1* and *Erg*$^{+/+}$ mock for each gene. (*K*) Model of ERG as a key regulator of HSC self-renewal versus differentiation. Data are represented as mean + SD. (w) Weeks. (ns) Not significant; (*) $P < 0.05$; (**) $P < 0.01$; (***) $P < 0.001$.

deficient leukemias displayed slightly longer latencies compared with controls, the differences were not dramatic—a fact paralleled by the normal T-cell development in *Erg*$^{fl/fl}$; *CD2iCre* animals (Fig. 7D–F).

To test whether ERG is equally dispensable for myeloid transformation, we transduced BM progenitors from *Erg*$^{fl/fl}$; *R26Cre-ER* mice with the potent myeloid oncogene *MLL-ENL* and subjected them to *Erg* deletion

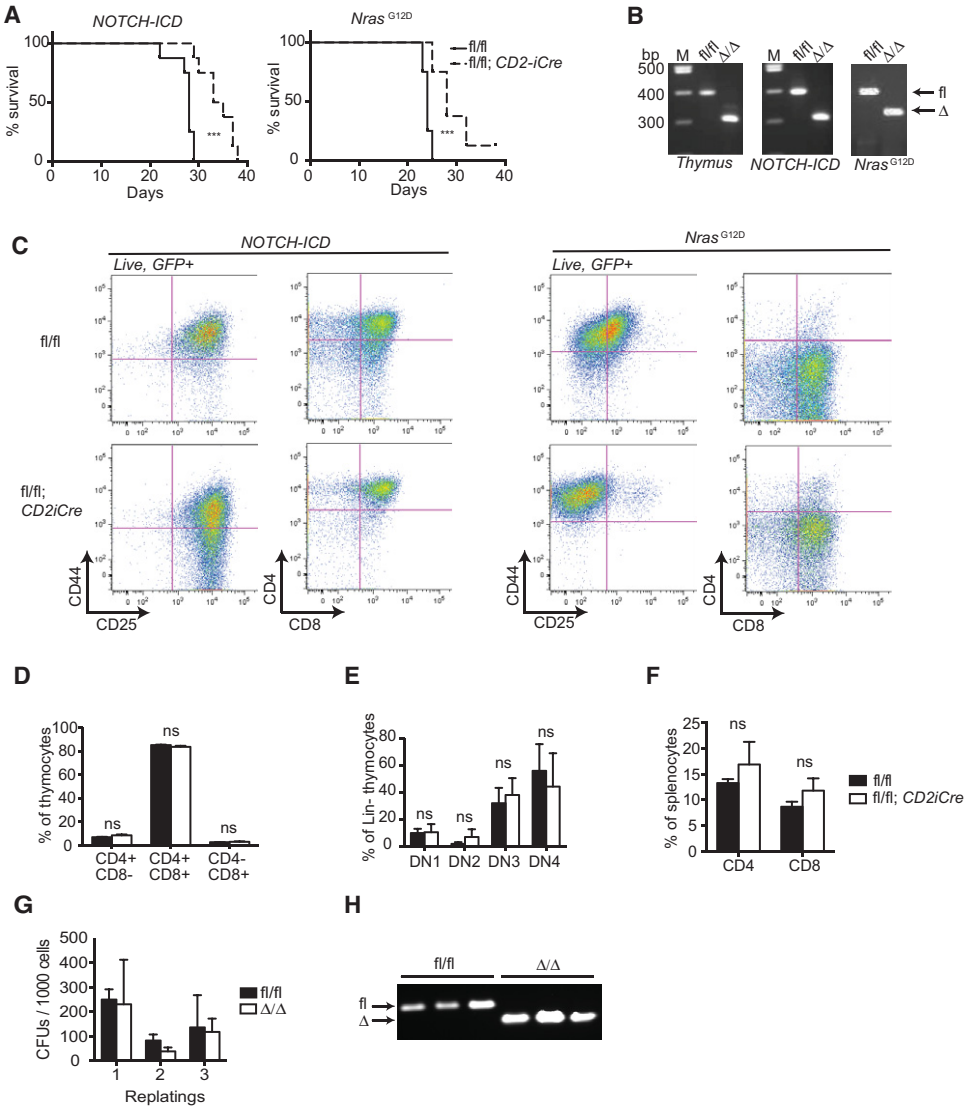

Figure 7. ERG is dispensable for both lymphoid and myeloid transformation. (*A*) Survival curves of recipients transplanted with $Erg^{fl/fl}$ ($n = 8$–12) or $Erg^{fl/fl}$; *CD2iCre* ($n = 8$) BM cells transduced with *NOTCH-ICD*-expressing or $Nras^{G12D}$-expressing retrovira. (*B*) Genotyping of thymi from normal $Erg^{fl/fl}$ and $Erg^{fl/fl}$; *CD2iCre* (Δ/Δ) mice as well as from T-ALLs developing in $Erg^{fl/fl}$ (fl/fl) or $Erg^{fl/fl}$; *CD2iCre* (Δ/Δ) mice. (*C*) FACS analysis of splenocytes derived from moribund recipients of BM cells transduced with *NOTCH-ICD*-expressing or $Nras^{G12D}$-expressing retrovirus (GFP^+). (*D*) FACS analysis was performed to quantify numbers of double-positive and single-positive thymocytes in normal $Erg^{fl/fl}$ ($n = 4$) and $Erg^{fl/fl}$; *CD2iCre* ($n = 4$) mice. (*E*) Quantification of thymic progenitors in $Erg^{fl/fl}$ ($n = 4$) and $Erg^{fl/fl}$; *CD2iCre* ($n = 4$) mice. (*F*) FACS analysis of mature CD4-expressing and CD8-expressing splenocytes in $Erg^{fl/fl}$ ($n = 4$) and $Erg^{fl/fl}$; *CD2iCre* ($n = 4$) mice. (*G*) Serial replating of *MLL-ENL* transformed $Erg^{fl/fl}$ ($n = 3$) and $Erg^{\Delta/\Delta}$ ($n = 3$) BM cells. (*H*) Genotyping of the cells from *G*. Data are represented as mean + SD. (ns) Not significant; (***) $P < 0.001$. (M) Marker; (DN) double negative.

with 4-OHT followed by serial replating in colony assays (Fig. 7G,H). Strikingly, but in line with the results from the T-ALL experiments, this surrogate assay of leukemic stem cell maintenance demonstrated no requirement for the presence of ERG. We therefore conclude that ERG is dispensable for both lymphoid and myeloid transformation. This excludes a general role for ERG in the maintenance of hematopoietic cells with stem-like properties such as leukemic stem cells, thus further highlighting its unique role within the normal HSC compartment.

Discussion

HSCs are endowed with the ability to sustain the lifelong production of hematopoietic cells. Crucial to this process is their ability to regulate the balance between self-renewal and differentiation such that HSC numbers are maintained while at the same time ensuring the sufficient production of mature blood cells.

Here we explored the function of the ETS factor ERG in HSCs. ERG has previously been found to be essential for fetal hematopoiesis and adult stress hematopoiesis in a

manner that appeared to converge at the inability of *Erg* mutant HSCs to expand in a variety of settings (Loughran et al. 2008; Ng et al. 2011; Taoudi et al. 2011). These earlier studies all used the Erg^{Mld2} allele that encodes an ERG variant with a mutation in the DNA-binding ETS domain. Although this mutant is inactive in reporter assays, it still binds DNA, thus raising the concern that it potentially could interfere with the function of other ETS proteins through binding to ETS consensus binding sites. To circumvent this problem, we generated an *Erg* mutant allele that facilitates the conditional deletion of the entire ETS domain, thus generating an ERG variant with no DNA-binding activity, which in turn allows us to study the specific role of ERG without any potential confounding impact on other ETS factors. Importantly, this model makes it possible to assess the impact of complete functional loss of ERG in an adult setting.

Using this newly developed conditional *Erg* knockout model, we found that ablation of ERG in adult mice leads to a complete loss of HSCs without any apparent changes in their proliferative or apoptotic behavior. Instead, kinetic analysis of HSCs and their immediate descendants following ERG ablation demonstrated that HSCs were depleted prior to the loss of MPPs. Moreover, mathematical modeling of the data is consistent with a model in which the loss of *Erg* leads to a >20-fold increase in the differentiation rate of HSCs, implying that ERG serves to restrict the differentiation of HSCs. Thus, our data add considerably to the earlier proposed function of ERG in HSCs, and, to our knowledge, this is the first example of a transcription factor that serves to restrict premature differentiation of HSCs.

Numerous studies have implicated the proto-oncogene *Myc* in the regulation of self-renewal and differentiation of HSCs. Thus, whereas conditional deletion of *Myc* in the hematopoietic system leads to a block in differentiation and accumulation of HSCs, overexpression of *Myc* is associated with HSC depletion and increased differentiation (Wilson et al. 2004). Importantly, none of these phenotypes was associated with any changes in HSC proliferation and apoptosis, and the *Myc* overexpression HSC phenotype therefore perfectly mirrors the loss of *Erg* in HSCs. Furthermore, we found that several previously reported MYC target gene signatures are up-regulated in *Erg*-deficient HSCs and that these are enriched for genes directly targeted by ERG in the HPC-7 HSC/HPC line. We therefore propose a model in which ERG represses the activity of some MYC target genes, thus restricting the MYC-driven differentiation of HSCs. According to this model, modulation of MYC and/or ERG function or levels would consequently affect the delicate balance of HSC self-renewal versus differentiation (Fig. 6K). Consistent with this model, we found that inhibition of MYC activity through the BET inhibitor CPI-203 in *Erg*-deficient mice is able to improve the HSC defect significantly, with stabilization of HSC levels in the BM of both $Erg^{\Delta/\Delta}$ and $Erg^{+/-}$ mice after only 1 wk of treatment. Similarly, HSCs from CPI-203-treated mice display improved functional properties with increased long-term multilineage engraftment of PB hematopoiesis compared with control, arguing that the balance again has been shifted back in favor of self-renewal. Of note, we do realize that *Myc* is not the only target of CPI-203 but is clearly one of those responding most efficiently to the drug, and previous studies have indicated that BET inhibitors appear to phenocopy genetic ablation of *Myc* (King et al. 2013; Loven et al. 2013). We therefore conclude that most of CPI-203's effects on HSC properties are due to modulation of MYC activity.

It is interesting to note that *Myc* repression also has a clear impact on wild-type HSCs where ERG levels are normal. These results indicate that lowering of MYC activity has an HSC-promoting effect independent of ERG status. This is compatible with the observations reported previously for *Myc*-null HSCs, which exhibit a dramatic block in differentiation. Nevertheless, these observations do not undermine the proposed role of ERG as a major HSC maintenance factor and do not exclude that ERG and MYC coregulate differentiation genes. Instead, we show that MYC targets that were up-regulated in *Erg*-deficient HSCs could be lowered upon *Myc* down-regulation, clearly arguing for a situation in which the combination of ERG and MYC controls the expression levels of certain differentiation-promoting genes.

Finally, in addition to its role as a modulator of MYC-induced gene expression, our gene expression analysis also demonstrated that ERG induces the expression of several genes previously identified as HSC self-renewal factors. ERG therefore emerges as a key HSC regulator, as it is involved in governing several aspects of HSC homeostasis.

Our work also offers novel insights into differences in the wiring of self-renewal/differentiation pathways between HSCs and leukemic cells. Thus, in contrast to the crucial role of ERG in the maintenance of normal HSCs, we found that ERG is essentially dispensable for the development of lymphoid leukemia as well as the transformation of myeloid cells into myeloid leukemia. These findings suggest that the leukemic stem cells responsible for the maintenance of both lymphoid and myeloid leukemias are not always dependent on normal self-renewal/survival pathways. High expression of *ERG* in both T-ALL and AML patients has been associated with an adverse prognosis, and *ERG* overexpression has been shown to drive the formation of both lymphoid and myeloid leukemias in mice (Marcucci et al. 2005, 2007; Baldus et al. 2006; Salek-Ardakani et al. 2009; Tsuzuki et al. 2011; Carmichael et al. 2012). The fact that ERG is implicated in tumors of both myeloid and lymphoid origin as well as the data described in the present work suggest a model in which the main role of *ERG* overexpression in patients is to expand the numbers of HSCs, presumably by restricting their differentiation. This may in turn render HSCs amenable to the acquisition of secondary mutations that ultimately drives leukemic transformation.

In summary, our work demonstrates that ERG plays different roles in normal HSCs and their leukemic counterparts. We propose a model in which ERG serves to restrict HSC differentiation by activating stem cell genes and repressing the expression of MYC target genes, thereby placing ERG at center stage in the regulation of the delicate balance between HSC self-renewal and differentiation.

Material and methods

Flow cytometry

BM (2× femur, tibia, and ilium) and spleens were collected and crushed in PBS and 3% fetal calf serum (FCS) (GE Healthcare). Cell suspensions were stained for mature cells using antibodies against Ter119, Mac-1, Gr-1, B220, CD4, and CD8a (eBioscience); myelo–erythroid progenitor cells using antibodies against lineage (CD3e, B220, Mac-1, and Gr-1), Sca-1, c-Kit, CD105, CD41, FcgRII/III, Ter119 (eBioscience), and CD150 (Biolegend); and HSCs/HPCs using antibodies against either B220, CD3, CD11b, Gr1, Ter119, Sca-1, c-Kit (eBioscience), CD150, and CD48 (Biolegend) (2- and 4-wk time points) or B220, CD3, CD11b, Gr1, Ter119, Sca-1, c-Kit (eBioscience), CD45 (BD), EPCR (Stem Cell Technologies), CD150, and CD48 (Biolegend) (1-wk time point). For the analysis of transplanted animals, antibody cocktails were supplemented with CD45.1 (eBioscience) and CD45.2 (BD) antibodies. After washing, stained cells were resuspended in PBS and 3% FCS containing 0.2 µg/mL DAPI (Invitrogen) or 1 µg/mL 7AAD (Invitrogen). For stem and progenitor cell purification, c-Kit$^+$ cells were enriched with anti-c-Kit beads by MACS (Miltenyi Biotec) prior to antibody staining. Red blood cells were removed by PharmLyse (BD) according to the manufacturers' protocol.

Thymi from 7- to 9-wk-old mice were stained using lineage-specific antibodies (Ter119, Mac1, Gr1, B220, CD19, NK1.1, CD3e, CD4, CD8, CD44 [eBioscience], and CD25 [BD]).

PB was stained for B220, CD4, CD8a, CD11b, CD45.1 (e-Bioscience), and CD45.2 (BD) as described (Hasemann et al. 2014) or was analyzed for haematological parameters using Advia120 (Siemens).

For analysis purposes, samples were run on an LSRII (BD), whereas cell sorting was performed on a FACS Aria (BD). The data were analyzed using FlowJo version 9 (TreeStar).

Transplantation assays

All transplantation assays were performed using the Ly-5 congenic mouse system.

For reciprocal transplantation, 3×10^6 Ly5.1 BM cells (CD45.1) were transplanted by tail vein injection into either irradiated (900 cGy) or nonirradiated $Erg^{fl/fl}$ or $Erg^{\Delta/\Delta}$ Ly-5.2 (CD45.2) mice 10 d after initiating pIpC treatment (five injections in total).

For transplantation with nondeleted donor cells, 4.5×10^6 BM cells from $Erg^{fl/fl}$ or $Erg^{fl/fl}$; *Mx1Cre* (CD45.2) mice were intravenously injected into irradiated (900 cGy) Ly-5.1 (CD45.1) recipients along with 5×10^5 CD45.1 competitor cells. Four months after transplantation, the blood chimerism was analyzed, and, 2 wk later, excision of *Erg* was induced with pIpC injections.

For whole BM competitive repopulation assays, 3×10^5 or 3×10^6 BM cells from $Erg^{fl/fl}$ or $Erg^{\Delta/\Delta}$ Ly-5.2 (CD45.2) mice (2 wk after excision of *Erg*) were mixed with 3×10^5 competitor BM cells Ly-5.1 (CD45.1) and transplanted by tail vein injection into lethally irradiated (900 cGy) Ly-5.1 (CD45.1) mice. For competitive transplantations of $Erg^{+/+}$ or $Erg^{+/-}$ BM, $2.5 \times 10^6 + 2.5 \times 10^6$ and $4.5 \times 10^6 + 0.5 \times 10^6$ cells were injected (1:1 and 10:1 donor:competitor ratio, respectively).

For HSC/MPP competitive repopulation assays, 30 freshly isolated HSCs (LSK CD150$^+$) or 150 MPPs (LSK CD150$^-$) from $Erg^{fl/fl}$ or $Erg^{\Delta/\Delta}$ Ly-5.2 (CD45.2) mice 2 wk after excision of *Erg* were mixed with 2×10^5 Ly-5.1 (CD45.1) competitor BM cells and transplanted by tail vein injection into irradiated (900 cGy) Ly-5.1 (CD45.1) mice.

Gene expression profiling

RNA was purified using the RNeasy microkit (Qiagen) from sorted $Erg^{+/-}$ and $Erg^{+/+}$ HSCs (LSK CD150$^+$ CD48$^-$) or $Erg^{\Delta/\Delta}$ and $Erg^{fl/fl}$ MPPs (LSK CD150$^-$) and subjected to microarray (Mouse Gene 1.0 ST GeneChip array, Affymetrix) as described in Hasemann et al. (2014). Microarray data were normalized by RMA (robust multiarray analysis) followed by mean one-step probe set summarization using the Partek genomics suite 6.5 followed by analysis of differential expression between experimental groups (expression fold change >1.5; $P < 0.05$; $q < 0.22$, ANOVA *F*-test). The raw data can be accessed at the Gene Expression Omnibus under accession number GSE69873.

For qRT–PCR, cDNA was synthesized by help of the ProtoScript first strand cDNA synthesis kit (New England Biolabs) with oligo-d(T) primers. qPCR was performed with LightCycler 480 SYBR Green I Master mix (Roche) and a Roche LightCycler 480 instrument using primers listed in the Supplemental Material. Gene expression levels were normalized to γ-actin (*Actg1*).

GSEA

GSEA was performed using GSEA version 4.0 (http://www.broadinstitute.org/gsea). Gene sets originated from the MSigDB (http://www.broadinstitute.org/gsea/msigdb) and a list of curated signatures extracted from Venezia et al. (2004), Mansson et al. (2007), and Pronk et al. (2007). The curated signatures were kindly provided by Susan Moore and Claus Nerlov.

ERG ChIP-seq data analysis

The ERG ChIP-seq data were obtained from Wilson et al. (2010), where summits from the union of called peaks between three peak callers were used for further analysis. We defined ERG-binding sites in a window of ±70 bp with respect to the summit positions. Genes from microarray analysis were deemed significantly differentially expressed using a fold change threshold of >1.5 ($P < 0.05$). Promoter regions (defined by TSS ± 800 bp, with sequences acquired from RefSeq mm9 assembly using the longest isoform) of differentially expressed genes were overlaid with ERG peaks. Using this union, the significance of overlap was calculated using a permutation test drawing

a similar sample size 10,000 times from random genes on the microarray.

De novo motif discovery among ERG peaks was performed using MEME-chip (Machanick and Bailey 2011). The frequency tables from DREME (matching against the JASPAR database) (Sandelin et al. 2004; Bailey 2011) was used as input to FIMO (Grant et al. 2011) to find significant occurrences of selected ERG CHIP-seq motifs within sequences of the differentially expressed genes ($P < 0.01$). Based on counts of these significant occurrences, the upper quartile of differentially expressed genes was overlapped with gene signatures from the MSigDB (C2, C5, and C6; hypergeometric test, $P < 0.05$).

AML and T-ALL analysis

To generate AML on an *Erg*-deficient background, c-Kit-enriched BM from $Erg^{fl/fl}$ and $Erg^{fl/fl}$; *R26-CreER* mice were transduced with *MLL-ENL-IRES-GFP* (Ohlsson et al. 2014) and transformed through three passages in colony assays (Stem Cell Technologies, M3231) supplemented with 100 U/mL penicillin, 100 µg/mL streptomycin, 20 ng/mL murine SCF (mSCF) (PeproTech), 10 ng/mL human IL-6 (hIL-6) (PeproTech), 10 ng/mL human GM-CSF, and 10 ng/mL murine IL-3 (PeproTech). $Erg^{fl/fl}$ and $Erg^{fl/fl}$; *R26-CreER* transformed colonies were subsequently dissociated and passaged in RPMI 1640 (Invitrogen) supplemented with 20% FCS, 20% WEHI-conditioned medium, 20 ng/mL mSCF, and 10 ng/mL hIL-6 ± 0.5 µM 4-OHT to allow for excision of *Erg*. Finally, serial replating assays were performed as described in Ohlsson et al. (2014). For T-ALL analysis, c-Kit-enriched BM from $Erg^{fl/fl}$ and $Erg^{fl/fl}$; *Cd2iCre* mice was transduced with *NOTCH-ICD* (Chiang et al. 2008) or $Nras^{G12D}$ in which luciferase was replaced with Venus (Zuber et al. 2009) and transplanted to irradiated (900 cGy) Ly5.1 recipients (CD45.1). Log rank test was used to analyze differences in survival.

Pharmacological targeting of Myc *expression*

CPI-203 (DC Chemicals) was dissolved in 0.9% saline solution, 5% DMSO (Sigma-Aldrich), and 10% hydroxypropyl-β-cyclodextrin (Sigma-Aldrich) and administered by intraperitoneal injection twice daily at 5 mg/kg. Mock-treated mice were injected with the corresponding volume of saline/DMSO/hydroxypropyl-β-cyclodextrin solution. Sorted LSK $CD150^+$ $CD48^-$ cells were cultured in StemSpan SFEM (Stem Cell Technologies) with 10% FCS, 100 U/mL penicillin, 100 µg/mL streptomycin, 100 ng/mL mSCF, and 0.5 µM CPI-203 or the corresponding volume of DMSO. C-Kit-enriched cells were cultured in IMDM with 10% FCS, 100 U/mL penicillin, 100 µg/mL streptomycin, 50 ng/mL mSCF, and 0.5 µM CPI-203 or the corresponding volume of DMSO. Cells were harvested after 24 h of culture, immediately dissolved in RLT lysis buffer from the RNeasy microkit, and stored at −80°C until further purification.

Statistical analyses

Student two-tailed *t*-test was used to test for significance throughout, unless specifically stated.

Acknowledgments

We thank Anna Fossum for help with cell sorting, and members of the Porse laboratory for discussions. This study was supported by grants from the Danish Cancer Society (A1007 and DP08059 to K.T.-M.), the Lundbeck Foundation (26130 and 29367 to K.T.-M.), and the NovoNordisk Foundation (34220 to K.T.-M.), and a Centre grant from the NovoNordisk Foundation (The NovoNordisk Foundation Section for Stem Cell Biology in Human Disease). K.T.-M. is supported by a clinical research fellowship from the Novo Nordisk Foundation (grant no. 35247). K.J.K., M.R., M.S.H., E.O., A.W., A.-K.F., E.S., J.J., L.T., and J.L. performed experiments. F.O.B., N.R., K.J.K., M.R., E.S., L.T., and J.L. analyzed data. K.J.K., M.R., L.T., J.L., K.T.-M., and B.T.P. designed experiments. K.T.-M. and B.T.P. directed research. M.R., M.S.H., and B.T.P. drafted the manuscript. All authors proofread and approved the final version of the manuscript.

References

Bailey TL. 2011. DREME: motif discovery in transcription factor ChIP-seq data. *Bioinformatics* **27:** 1653–1659.

Baldus CD, Burmeister T, Martus P, Schwartz S, Gokbuget N, Bloomfield CD, Hoelzer D, Thiel E, Hofmann WK. 2006. High expression of the ETS transcription factor ERG predicts adverse outcome in acute T-lymphoblastic leukemia in adults. *J Clin Oncol* **24:** 4714–4720.

Carmichael CL, Metcalf D, Henley KJ, Kruse EA, Di Rago L, Mifsud S, Alexander WS, Kile BT. 2012. Hematopoietic overexpression of the transcription factor Erg induces lymphoid and erythro-megakaryocytic leukemia. *Proc Natl Acad Sci* **109:** 15437–15442.

Challen GA, Sun D, Jeong M, Luo M, Jelinek J, Berg JS, Bock C, Vasanthakumar A, Gu H, Xi Y, et al. 2012. Dnmt3a is essential for hematopoietic stem cell differentiation. *Nat Genet* **44:** 23–31.

Chiang MY, Xu L, Shestova O, Histen G, L'Heureux S, Romany C, Childs ME, Gimotty PA, Aster JC, Pear WS. 2008. Leukemia-associated NOTCH1 alleles are weak tumor initiators but accelerate K-ras-initiated leukemia. *J Clin Invest* **118:** 3181–3194.

Essers MA, Offner S, Blanco-Bose WE, Waibler Z, Kalinke U, Duchosal MA, Trumpp A. 2009. IFNα activates dormant haematopoietic stem cells in vivo. *Nature* **458:** 904–908.

Goldberg L, Tijssen MR, Birger Y, Hannah RL, Kinston SJ, Schutte J, Beck D, Knezevic K, Schiby G, Jacob-Hirsch J, et al. 2013. Genome-scale expression and transcription factor binding profiles reveal therapeutic targets in transgenic ERG myeloid leukemia. *Blood* **122:** 2694–2703.

Grant CE, Bailey TL, Noble WS. 2011. FIMO: scanning for occurrences of a given motif. *Bioinformatics* **27:** 1017–1018.

Hasemann MS, Lauridsen FK, Waage J, Jakobsen JS, Frank AK, Schuster MB, Rapin N, Bagger FO, Hoppe PS, Schroeder T, et al. 2014. C/EBPα is required for long-term self-renewal and lineage priming of hematopoietic stem cells and for the maintenance of epigenetic configurations in multipotent progenitors. *PLoS Genet* **10:** e1004079.

Ichikawa M, Asai T, Saito T, Seo S, Yamazaki I, Yamagata T, Mitani K, Chiba S, Ogawa S, Kurokawa M, et al. 2004.

AML-1 is required for megakaryocytic maturation and lymphocytic differentiation, but not for maintenance of hematopoietic stem cells in adult hematopoiesis. *Nat Med* **10:** 299–304.

Ichikawa M, Goyama S, Asai T, Kawazu M, Nakagawa M, Takeshita M, Chiba S, Ogawa S, Kurokawa M. 2008. AML1/Runx1 negatively regulates quiescent hematopoietic stem cells in adult hematopoiesis. *J Immunol* **180:** 4402–4408.

Iwama A, Oguro H, Negishi M, Kato Y, Morita Y, Tsukui H, Ema H, Kamijo T, Katoh-Fukui Y, Koseki H, et al. 2004. Enhanced self-renewal of hematopoietic stem cells mediated by the polycomb gene product Bmi-1. *Immunity* **21:** 843–851.

King B, Trimarchi T, Reavie L, Xu L, Mullenders J, Ntziachristos P, Aranda-Orgilles B, Perez-Garcia A, Shi J, Vakoc C, et al. 2013. The ubiquitin ligase FBXW7 modulates leukemia-initiating cell activity by regulating MYC stability. *Cell* **153:** 1552–1566.

Ko M, Bandukwala HS, An J, Lamperti ED, Thompson EC, Hastie R, Tsangaratou A, Rajewsky K, Koralov SB, Rao A. 2011. Ten-eleven-translocation 2 (TET2) negatively regulates homeostasis and differentiation of hematopoietic stem cells in mice. *Proc Natl Acad Sci* **108:** 14566–14571.

Lieu YK, Reddy EP. 2009. Conditional c-myb knockout in adult hematopoietic stem cells leads to loss of self-renewal due to impaired proliferation and accelerated differentiation. *Proc Natl Acad Sci* **106:** 21689–21694.

Loughran SJ, Kruse EA, Hacking DF, de Graaf CA, Hyland CD, Willson TA, Henley KJ, Ellis S, Voss AK, Metcalf D, et al. 2008. The transcription factor Erg is essential for definitive hematopoiesis and the function of adult hematopoietic stem cells. *Nat Immunol* **9:** 810–819.

Loven J, Hoke HA, Lin CY, Lau A, Orlando DA, Vakoc CR, Bradner JE, Lee TI, Young RA. 2013. Selective inhibition of tumor oncogenes by disruption of super-enhancers. *Cell* **153:** 320–334.

Machanick P, Bailey TL. 2011. MEME-ChIP: motif analysis of large DNA datasets. *Bioinformatics* **27:** 1696–1697.

Mansson R, Hultquist A, Luc S, Yang L, Anderson K, Kharazi S, Al-Hashmi S, Liuba K, Thoren L, Adolfsson J, et al. 2007. Molecular evidence for hierarchical transcriptional lineage priming in fetal and adult stem cells and multipotent progenitors. *Immunity* **26:** 407–419.

Marcucci G, Baldus CD, Ruppert AS, Radmacher MD, Mrozek K, Whitman SP, Kolitz JE, Edwards CG, Vardiman JW, Powell BL, et al. 2005. Overexpression of the ETS-related gene, ERG, predicts a worse outcome in acute myeloid leukemia with normal karyotype: a Cancer and Leukemia Group B study. *J Clin Oncol* **23:** 9234–9242.

Marcucci G, Maharry K, Whitman SP, Vukosavljevic T, Paschka P, Langer C, Mrozek K, Baldus CD, Carroll AJ, Powell BL, et al. 2007. High expression levels of the ETS-related gene, ERG, predict adverse outcome and improve molecular risk-based classification of cytogenetically normal acute myeloid leukemia: a Cancer and Leukemia Group B Study. *J Clin Oncol* **25:** 3337–3343.

Moran-Crusio K, Reavie L, Shih A, Abdel-Wahab O, Ndiaye-Lobry D, Lobry C, Figueroa ME, Vasanthakumar A, Patel J, Zhao X, et al. 2011. Tet2 loss leads to increased hematopoietic stem cell self-renewal and myeloid transformation. *Cancer Cell* **20:** 11–24.

Ng AP, Loughran SJ, Metcalf D, Hyland CD, de Graaf CA, Hu Y, Smyth GK, Hilton DJ, Kile BT, Alexander WS. 2011. Erg is required for self-renewal of hematopoietic stem cells during stress hematopoiesis in mice. *Blood* **118:** 2454–2461.

Ohlsson E, Hasemann MS, Willer A, Lauridsen FK, Rapin N, Jendholm J, Porse BT. 2014. Initiation of MLL-rearranged AML is dependent on C/EBPα. *J Exp Med* **211:** 5–13.

Pronk CJ, Rossi DJ, Mansson R, Attema JL, Norddahl GL, Chan CK, Sigvardsson M, Weissman IL, Bryder D. 2007. Elucidation of the phenotypic, functional, and molecular topography of a myeloerythroid progenitor cell hierarchy. *Cell Stem Cell* **1:** 428–442.

Quivoron C, Couronne L, Della Valle V, Lopez CK, Plo I, Wagner-Ballon O, Do Cruzeiro M, Delhommeau F, Arnulf B, Stern MH, et al. 2011. TET2 inactivation results in pleiotropic hematopoietic abnormalities in mouse and is a recurrent event during human lymphomagenesis. *Cancer Cell* **20:** 25–38.

Rodrigues NP, Janzen V, Forkert R, Dombkowski DM, Boyd AS, Orkin SH, Enver T, Vyas P, Scadden DT. 2005. Haploinsufficiency of GATA-2 perturbs adult hematopoietic stem-cell homeostasis. *Blood* **106:** 477–484.

Rosen P, Sesterhenn IA, Brassell SA, McLeod DG, Srivastava S, Dobi A. 2012. Clinical potential of the ERG oncoprotein in prostate cancer. *Nat Rev Urol* **9:** 131–137.

Rossi L, Lin KK, Boles NC, Yang L, King KY, Jeong M, Mayle A, Goodell MA. 2012. Less is more: unveiling the functional core of hematopoietic stem cells through knockout mice. *Cell Stem Cell* **11:** 302–317.

Salek-Ardakani S, Smooha G, de Boer J, Sebire NJ, Morrow M, Rainis L, Lee S, Williams O, Izraeli S, Brady HJ. 2009. ERG is a megakaryocytic oncogene. *Cancer Res* **69:** 4665–4673.

Sandelin A, Alkema W, Engstrom P, Wasserman WW, Lenhard B. 2004. JASPAR: an open-access database for eukaryotic transcription factor binding profiles. *Nucleic Acids Res* **32:** D91–D94.

Taoudi S, Bee T, Hilton A, Knezevic K, Scott J, Willson TA, Collin C, Thomas T, Voss AK, Kile BT, et al. 2011. ERG dependence distinguishes developmental control of hematopoietic stem cell maintenance from hematopoietic specification. *Genes Dev* **25:** 251–262.

Tsuzuki S, Taguchi O, Seto M. 2011. Promotion and maintenance of leukemia by ERG. *Blood* **117:** 3858–3868.

Venezia TA, Merchant AA, Ramos CA, Whitehouse NL, Young AS, Shaw CA, Goodell MA. 2004. Molecular signatures of proliferation and quiescence in hematopoietic stem cells. *PLoS Biol* **2:** e301.

Wei GH, Badis G, Berger MF, Kivioja T, Palin K, Enge M, Bonke M, Jolma A, Varjosalo M, Gehrke AR, et al. 2010. Genome-wide analysis of ETS-family DNA-binding in vitro and in vivo. *EMBO J* **29:** 2147–2160.

Will B, Vogler TO, Bartholdy B, Garrett-Bakelman F, Mayer J, Barreyro L, Pandolfi A, Todorova TI, Okoye-Okafor UC, Stanley RF, et al. 2013. Satb1 regulates the self-renewal of hematopoietic stem cells by promoting quiescence and repressing differentiation commitment. *Nat Immunol* **14:** 437–445.

Wilson A, Murphy MJ, Oskarsson T, Kaloulis K, Bettess MD, Oser GM, Pasche AC, Knabenhans C, Macdonald HR, Trumpp A. 2004. c-Myc controls the balance between hematopoietic stem cell self-renewal and differentiation. *Genes Dev* **18:** 2747–2763.

Wilson NK, Foster SD, Wang X, Knezevic K, Schutte J, Kaimakis P, Chilarska PM, Kinston S, Ouwehand WH, Dzierzak E, et al. 2010. Combinatorial transcriptional control in blood stem/progenitor cells: genome-wide analysis of ten major transcriptional regulators. *Cell Stem Cell* **7:** 532–544.

Zuber J, Radtke I, Pardee TS, Zhao Z, Rappaport AR, Luo W, McCurrach ME, Yang MM, Dolan ME, Kogan SC, et al. 2009. Mouse models of human AML accurately predict chemotherapy response. *Genes Dev* **23:** 877–889.